Biomedical Engineering, Vol. 11, No. 1, 2014

ROLE OF CONNECTIVITY AND CLUSTERS IN SPATIAL CYCLIC SIRS EPIDEMIC DYNAMICS

Ken A. Hawick
Department of Computer Science, University of Hull, Cottingham Road, Hull HU6 7RX, UK.
Email: k.a.hawick@hull.ac.uk, Tel: +44 01482 465181 Fax: +44 01482 466666

ABSTRACT

Understanding infection propagation and sustainability behaviours of epidemics in spatially distributed populations remain difficult problems. We use an agent-based simulation to explore the roles of geometrical agent connectivity and component clusters in the Susceptible, Infected, Recovered; Susceptible cyclic SIRS model. We study the distribution of sizes of infected clusters on simple nearest neighbour connected systems as well as other connectivity geometries including a Moore neighbourhood and a radial proximity connectivity. We find that both recovery probability and neighbourhood connectivity size affect and shift the infection probability trends and lead to increased sustainability of a system wide epidemic. We discuss the implications for managing the health of large spatial populations, the statistics of large scale epidemics and the effect of more realistic system geometries.

KEY WORDS

Population health modelling; SIRS cyclic model; agent-based model.

1 Introduction

Managing the spread of infections and the consequent dynamics of spatial epidemics [2, 5] is an ongoing and important problem in health informatics. Whilst great progress has been made in studying epidemic dynamics [18, 23] analytically [27] a spatial agent-based model allows investigation of emergent effects on a macroscopic spatial scale.

Agent-based approaches to spatial spread has been successful for modelling predator-prey systems [1, 4] using both analytical techniques [7, 19] and stochastic approaches [12,14,24]. Other models based on a spatial agent based approach with a contact infection process [21,22,28] have also successfully captured large scale agent population effects and behaviours whilst being formulated only in terms of microscopic individual agent parameters.

The well known susceptible-infected-recovered (SIR) epidemic model [29, 32] has been widely studied both analytically and spatially. A less studied alternative however is the cyclic SIRS model [30] which allows recovered agents to become re-susceptible to infection - and hence help sustain the spread of infection and potentially the life-cycle of an epidemic. Cyclic effects can have subtle but dramatic effects on the emergent spatial behaviour of agent-based models. Cyclic effects [10, 11] in the context of the SIRS model mean that we can study the nature of the dynamic equilibrium and the emergent spatial structure [8, 9] without agent populations crashing, which can of course occur if agents die or if, for example, there are no susceptible agents left as they have all recovered as occurs in the SIR model.

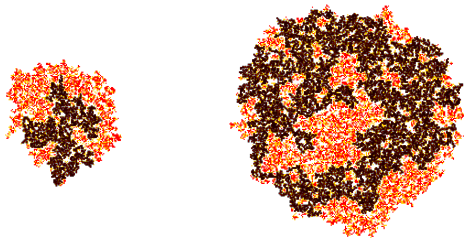

Figure 1. Spreading epidemic model snapshots with $\tau = \epsilon = 0.3; p = 1, t = 100, 200$, with largest infected cluster shown in black.

In this present article we study the SIRS model on a lattice [25, 26]. Agents eventually recover from infection in this model and can also become re-susceptible to infection again later. The total population size therefore remains steady. We believe our new contribution concerns study of the behaviour with different neighbourhood geometries and to this end, we couple the infection probability to the neighbourhood size of each individual agent so it is more likely that cross infection occurs if an agent has more infected neighbours. In effect the model time-step approximates the probabilistic events that might occur to an individual over a fixed time period such as a day - effectively integrating over many detailed interactions. Some work has been reported on the importance of household [13] and locality effects of this nature.

Much work has been reported in the literature on the formation and spread of an epidemic. Figure 1 shows a typical spatial infection model with susceptible sites in white, red infected sites, orange recovered sites and the largest infected cluster highlighted in black. In our present article we focus on the sustainability of an epidemic. We present results that the model system tends towards a dynamic equilibrium [15] infection rate - that is relatively independent

DOI: 10.2316/J.2014.216.815-0025

of the detailed individual initial conditions.

We analyse cluster and structural metrics such as the largest infected component size. These cluster metrics have not been widely studied [31] previously in this context but do help identify critical values [16] in the model parameter space, that are likely related to percolation thresholds [3,6].

Our article is structured as follows: In Section 2 we describe the SIRS model and how it is implemented as a spatial system using stochastic discrete events and agent-based modelling techniques. We present various illustrative model snapshots in Section 3 as well as various parametric plots showing the effects of infection and recovery parameters as well as the use of differing geometric connectivities. In Section 4 we discuss the implications of small and large infected component formation in the system for managing spatial epidemics. We offer some conclusions and suggested areas for further study in Section 5.

2 Simulation Method

We consider a lattice $\mathcal{L}$ of N sites which will typically be arranged in a square geometry of $N = L^2$ agents with one agent occupying a single site. In our present model every site is occupied and we do not simulate agents moving around. This localised agent model is a starting point that could be used to study the more complex case where agents can move locally or over long distances.

We are particularly interested in the effect of varying the agent connectivity neighbourhood $\mathcal{N}$ and its size $|\mathcal{N}|$. We restrict our attention in this present article to two dimensional connectivity arrangements on regular square lattice but we consider nearest neighbour, Moore neighbourhood and a proximity connectivity whereby any agent with a fixed radius is considered to be a connected neighbour. Only neighbouring agents can affect one another and in the SIRS model infected sites can infect any of the connected neighbours.

Prior work on the SIRS model [30] has used a fixed infection probability but we modify this so that it incorporates the neighbourhood size $|\mathcal{N}|$ so we can study a more realistic effect from changing the connectivity geometry.

Our lattice is then populated with agents whose individual states are: **S**usceptible; **I**nfected; or **R**ecovered and in contrast to the usual SIR model, where once agents are recovered they are considered permanently immune, we consider the more general SIRS case where recovered agents can become susceptible once again after some time.

The update algorithm for the SIRS model is cyclic so that:

$$S \xrightarrow{W_{SI}} I \xrightarrow{W_{IR}} R \xrightarrow{W_{RS}} S \qquad (1)$$

with rate parameters: $W_{SI} = p/|\mathcal{N}|$ governing the autocatalytic process of site potentially being infected by any infectious neighbour; $W_{IR} = \tau$ controlling spontaneous recovery; and $W_{RS} = \epsilon$ controlling the probability of recovered sites spontaneously becoming susceptible again. A useful starting point is to consider $\tau = \epsilon = 0.1$ before we scan the whole parameter space of the SIRS model. Clamping $\epsilon = 0$ recovers the non cyclic SIR model.

Algorithm 1 Cyclic SIRS Epidemic Agent Model.

```
choose lattice size, shape, eg square 64^2
choose neighbourhood N: Nearest, Moore, or Radial
for all runs eg 1..15 do
  initialise N agent sites as S, I, R uniformly
  for all time steps, eg 2,000 do
    for all agents i ∈ N in random order do
      if agent was Susceptible then
        count number n of infected neighbours
        infect it with probability p.n/|N|
      end if
      if agent was Infected then
        become Recovered with probability τ
      end if
      if agent was Recovering then
        become re-Susceptible with probability ε
      end if
    end for
    record measurements, eg cluster statistics
  end for
end for
normalise averaged measurements, and std. dvn.
```

We thus have a stochastic agent-based model with just two parameters considered in this present article. The simulation algorithm is summarised in Algorithm 1.

It is straightforward to count the numbers N_S, N_I, N_R of S, I, R agents and hence derive the normalised population fractions f_S, f_I and f_R. These are computationally cheap measurements to make upon the model. We also study the component cluster statistics of the model systems. Components can be labelled using various algorithms such as breadth first traversal of component labels. The system once labelled can be subsequently analysed and the clusters sorted and the largest identified. Typically this is a more computationally expensive process but we perform this for each time step to ensure we obtain representative average behaviours of the model. In the experiments reported we typically average over at least fifteen independent runs. This appears to attain satisfactorily small error-bars obtained from standard deviations of the measurements.

3 Selected Simulation Results

We present a number of screen-dump images illustrating the model behaviour as well as some plots of metrics averaged over several runs with independently seeded initial configurations of the model. Unlike some complex systems models, the SIRS model does not exhibit any particular need for very large systems to capture different length scale behaviours for example. Consequently, we show images for models with 256^2 sites, but present statistical averages over metrics for systems of size 64^2 sites.

Figure 2 shows screen shots illustrating different equilibrium configurations of the model for fixed values of

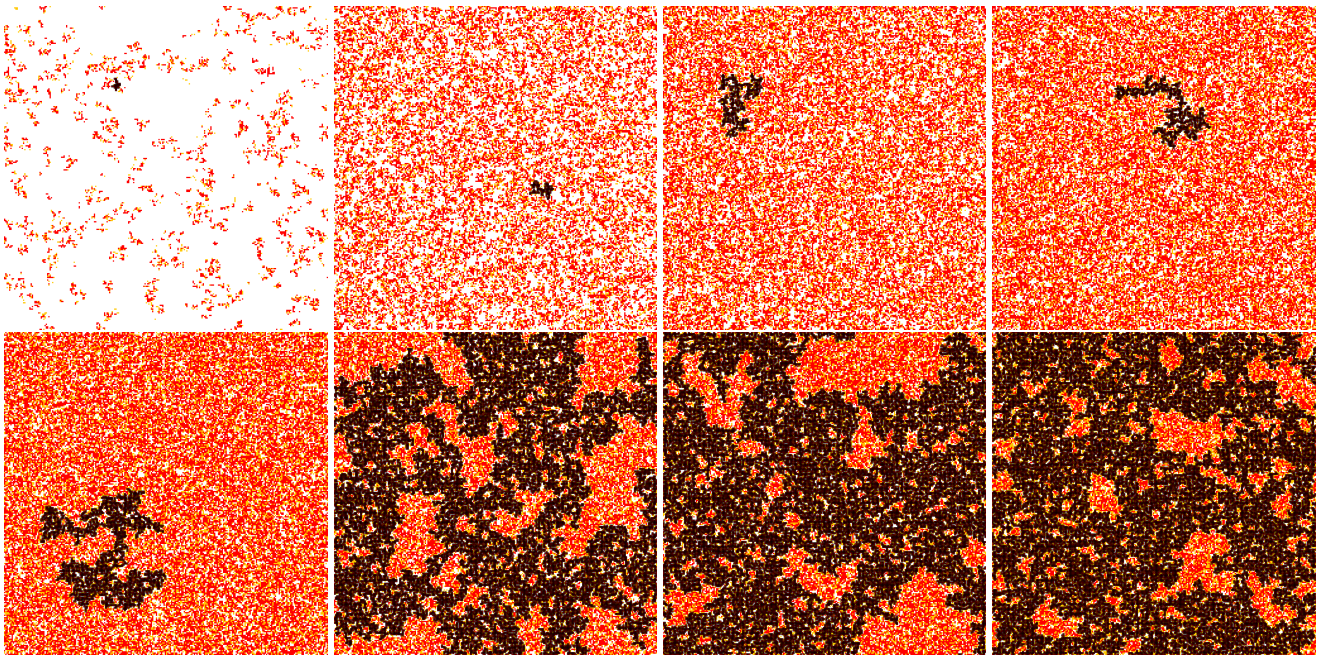

Figure 2. Screen-shots with $\tau = \epsilon = 0.1; p = 0.2, 0.3, 0.4, 0.5, 0.6, 0.7, 0.8, 0.9$ showing susceptible sites in white, red infected sites, orange recovered sites and the largest cluster of infected sites in black.

$\epsilon = tau = 0.1$ but for a range of the contact infection probability parameter p. These are for a simple nearest neighbour connectivity on a square lattice and with each site having four nearest neighbours. The model has been initialised with a random uniform mix of susceptible, infected and recovered individuals. At very low p the epidemic dies out and the system rapidly converges to a "white" system where all agents are susceptible. As p is increased to around 0.2 a dynamic equilibrium arises where there are enough infected sites to maintain a finite population of both infected and hence also recovered sites. The spatial clusters shown as red for infected and orange for recovered are generally quite small however. In effect the infected regions are localised. There is - as one might expect - a critical infection probability above which the epidemic maintains itself, and below which it will die out eventually.

It is interesting to study the cluster size and we show the largest cluster of infected sites in black. As p is increased we can see that the largest cluster remains quite small up to and including $p \approx 0.6$ but above this is effectively percolated. The site percolation threshold for square site lattice is around this value although since the model has three species and not just two, the value we obtain is somewhat higher than for simple 2-species site percolation.

We observe that above this value the black largest cluster spans the whole system. For simplicity of implementation we have used periodic boundary conditions on our simulation. This does not affect the qualitative behaviour but simply modifies the precise numerical values for the thresholds over those obtained for a finite open

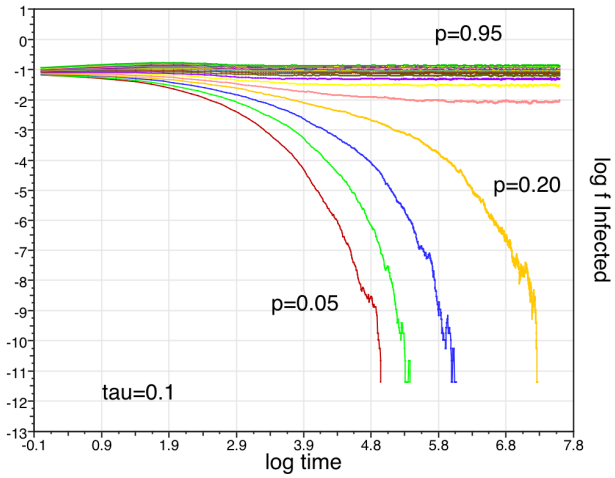

Figure 3. Time evolution of the fraction of agents currently infected.

boundary system. In this present article we are more interested in the qualitative regimes of the model than exact statistical values.

We can track various metrics computed for the model and this is valuable to see how the microscopic infection parameter p affects the behaviour of the systems as a whole.

Figure 3 shows the fraction of infected sites f_I plotted against simulation time on a log-log scale. This confirms the critical change in behaviour as p is increased. Below $p \approx 0.25$ f_I falls off after a time and the epidemic has died

out. It would be possible to study exactly how long this takes for a specific site infection geometry.

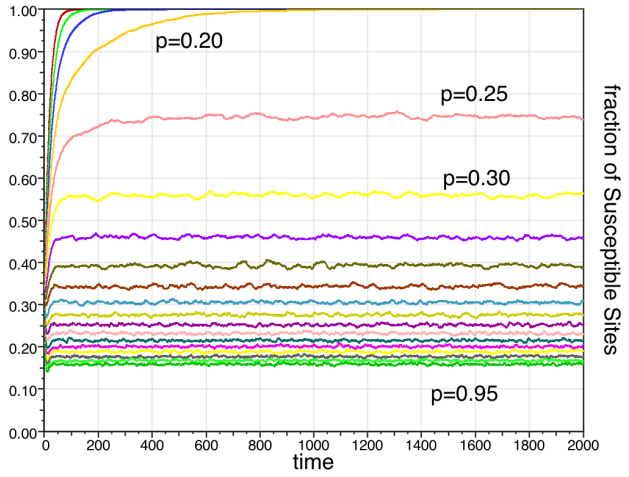

Figure 4. Time evolution of the fraction of agents currently susceptible to infection.

Figure 4 shows the corresponding fraction of susceptible sites but on a linear scale. This emphasises the nature of the dynamic equilibrium. The curves reach a dynamic equilibrium value about which they fluctuate - for our model it would appear this is reached after around 500 time steps. To ensure we are definitely measuring final values that were not contaminated by transients we measured final mean values averaging over the final 500 steps of a 2000 step run.

We can track the final equilibrium values of the f_S metric for variations in both $\tau = \epsilon$ and p and these are shown in Figure 5. We observe a large plateau region of $\tau - p$ parameter space where the epidemic has died out. The interesting regime is around low τ or high p. The simple plots shown above were for a fixed value of $\tau = 0.1$ but we see how modifying the recovery parameter τ only slightly, effectively shifts the p curves around.

To understand what is happening in the complex system it is useful to look at metrics that capture the component cluster behaviours.

Figure 6 shows plots of the number of connected components of infected sites plotted against simulation time on a log-log scale to equally emphasise the various scales. We see again the critical drop off phenomena for low infection parameter p but also a crossover at low times. At an early stage of the simulation high p actually leads to a initial drop in numbers of infected components that is more severe for high p than for low p. However after a knockout period this situation reverses and high p systems stabilise to a dynamic equilibrium value of number of infected components and low p system completely recover.

This behaviour can be seen more clearly in Figure 7 which shows the size of the largest infected cluster as a

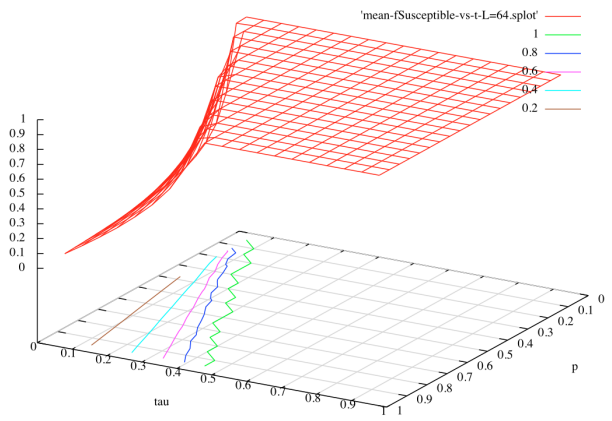

Figure 5. Parametric plot for the fraction of agents currently susceptible to infection.

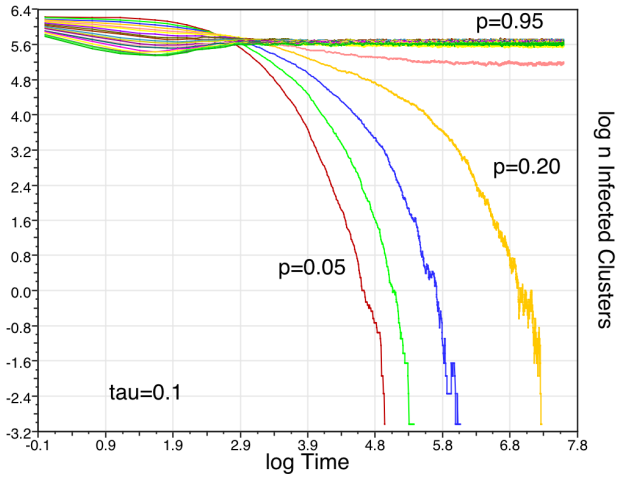

Figure 6. Time evolution of the number of infected components.

function of simulation time, again plotted on a log-log scale. The largest cluster initially rises for randomly initialised high p systems before reaching a dynamic equilibrium value whereas for low p systems in monotonically declines (apart from fluctuations) leading to a halting of the epidemic and all sites recovering.

We can examine how the recovery parameter τ changes this behaviour and the two dimensional parametric plots in Figure 8 and Figure 9 show the variation of the number of infected components and size of the largest infected component respectively.

In Figure 8 we see a shoulder pattern at low τ that shifts the p curves as discussed above. Generally values of $\tau < 0.4$ are non trivial. Above this the plateau regime of completely recovered agents is observed.

More detail on the shoulder regime at low p, τ can be discerned in Figure 9 which illustrates how the size of the

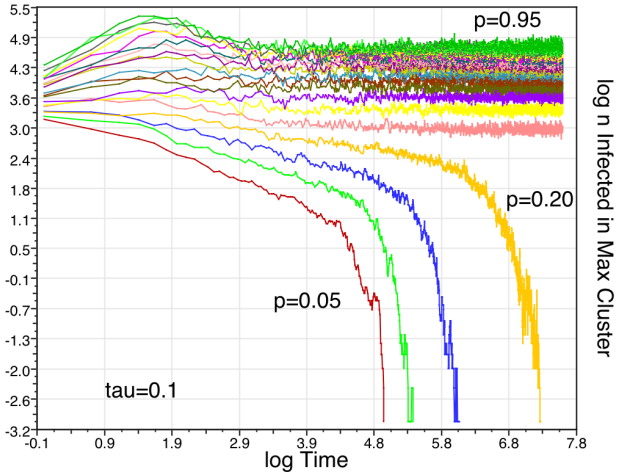

Figure 7. Time evolution of the size of the largest infected cluster.

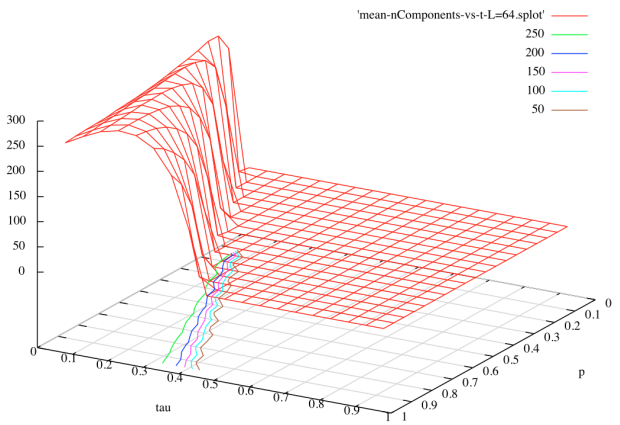

Figure 8. Parametric plot showing effect of infection probability and recovery probability on number of infected component clusters.

largest infected cluster size changes. Interestingly when the p behaviour is convex, the τ behaviour is concave. Again, raising the spontaneous probability of recovering (and becoming susceptible again) makes it easier for the epidemic to burn itself out and to fail to establish large spatial clusters of infected sites that can maintain the epidemic even with relatively high infection probability.

4 Discussion

Although this is a theoretical model without realistic geometrical details of a real environment, we can adjust the connectivity geometry to see how this affects the statistics of infection and recovery.

Figure 10 shows the variation of the fraction of infected sites against infection parameter p for fixed recovery parameter $\tau = \epsilon = 0.1$, but for three different connectivity geometries: nearest-neighbour (4); Moore neighbourhood(8); and radial proximity 4 with 48 neighbouring sites. Changing the number of neighbours shifts the cliff edge of the wholly-recovered plateau over. The curves presented have error bars of similar scale to the plot symbols and are relatively smooth.

We see somewhat more dramatic changes when we examine the corresponding curves for the number of infected component clusters and the size of the largest infected cluster.

Figure 11 shows that increasing the number of neighbours from four (nearest only) to eight (Moore neighbourhood) causes a quite substantive drop in the number of infected components.

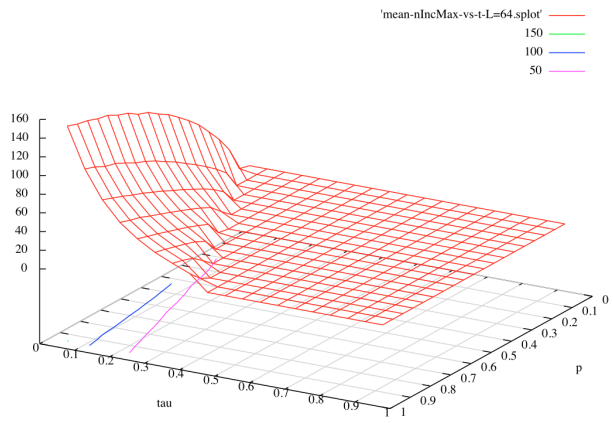

Figure 9. Parametric plot showing effect of infection probability and recovery probability on size of the largest cluster of infected agents.

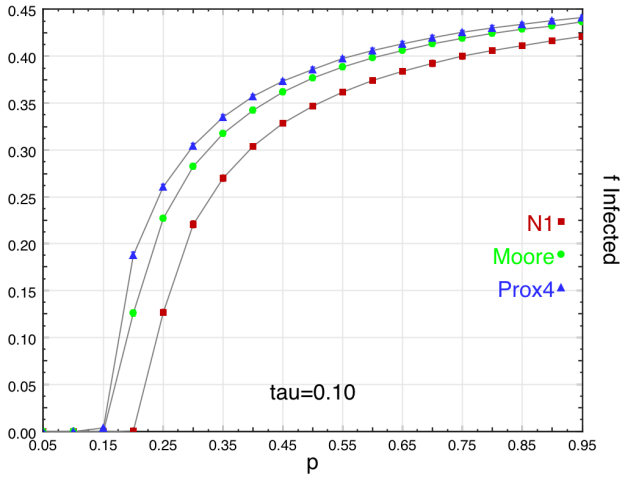

Figure 10. Final dynamic equilibrium fraction of infected sites plotted against infection parameter p for nearest-neighbour; Moore neighbourhood; and radial proximity 4 neighbourhoods.

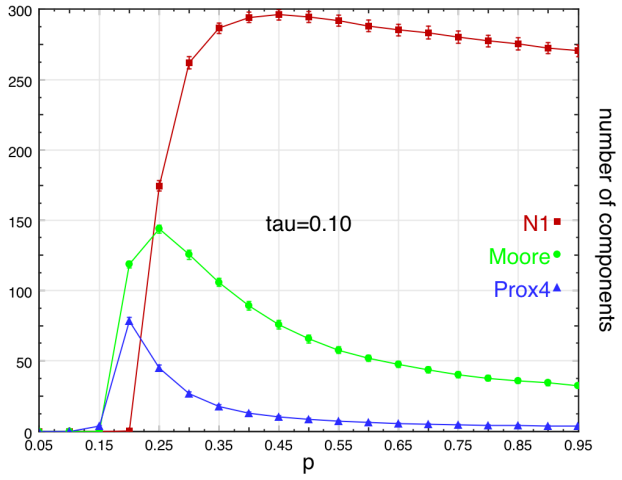

Figure 11. Number of infected components plotted against infection probability for different connectivity neighbourhoods.

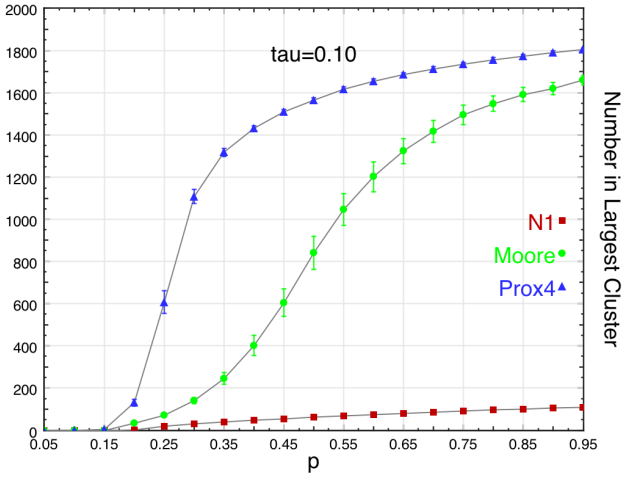

Figure 12. Size of largest infected cluster plotted against infection probability p for different connectivity neighbourhoods.

This manifests itself in the size of the largest infected component as shown in Figure 12 where we see an increase by nearly two orders of magnitude between systems with nearest neighbour and radial proximity connectivity.

A large connected cluster of infected sites will sustain itself for longer and the epidemic would persist for relatively low individual infection rates.

Figure 13 shows the parametric space and the effect of both infection parameter p and recovery parameter τ on the number of infected component clusters. We see a sharpening of the shoulder effect into a ridge as recovery probability is increased. For a highly connected system behaviour is dominated by the one infected super-cluster and even if the infection parameter can be lowered somehow the epidemic is likely to sustain itself.

Connectivity affects component cluster size and the effective spatial reach of the epidemic. Other spatial effects such as waves of infection [17] might also play a part in the sustainability of an epidemic. There is scope to study this using synchronous agent update algorithms. To avoid introducing accidental spatial artifacts we have erred on the side of caution and used an asynchronous agent update scheme for this present work and in fact have updated in a random order especially to avoid introducing accidental patterns. A cellular automata approach where all agents are updated at once could be used to deliberately allow waves and other correlation effects to persist and to see if these play a significant role in sustaining the epidemic spatial patterns.

Other detailed geometrical arrangements are possible and more specific network patterns [33] such as roads, transport links or other geographically realistic details could be explored. We believe these can be interesting but that it is valuable and important to explore the bulk statistical properties of a simple and spatially unbiased model first. Without doing so pathological features that are solely due to geographic details can be mistaken for normal emergent model properties.

The role of long range connections or "small world" graph connections [20] in epidemic models is also important. It is likely that the presence of many such small world connections transforms or bluntens the sharp phase transitional effects seen in the model into a smoother behaving system - albeit with perhaps faster infection spread. Such small work systems can sometimes be modelled analytically using mean-field techniques, and in some ways the spatial details then become less crucial.

Our model is highly localised, although as we have seen, increasing the size of the neighbourhood locality has a significant effect in sharpening the structure of the parametric space.

We have fixed the probability of becoming susceptible to be equal to the probability of recovery. We found the statistical behaviour of the fraction of recovered agents to be similar to the fraction of infected agents. A third independent parameter could be introduced into the model by making $\epsilon \neq \tau$ and experimenting to see if an independent spatial structure of recovered agents arises.

5 Conclusion

We have described the cyclic SIRS model and shown how it can be implemented as a discrete stochastic agent-based model on a lattice with various different neighbourhood connectivity geometries. We parameterised the model with spontaneous rate-equation based parameters for recovery and re-susceptibility. We used a normalised rate parameter for infection that incorporates the number of infected neighbours to make this contact process more realistic and coupled to the number of neighbouring agents impinging on a susceptible site.

The SIRS model tends towards a dynamical equi-

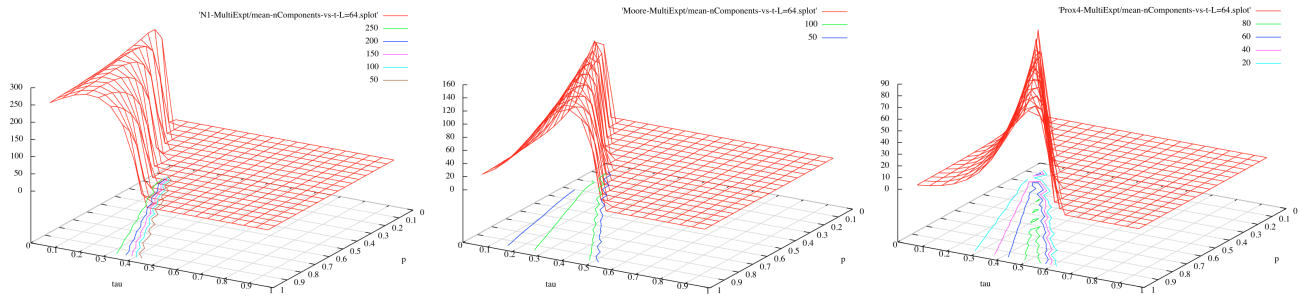

Figure 13. Number of Infected components for the $p - \tau$ parametric space, for nearest neighbour connectivity (left); Moore neighbourhood connectivity (middle) and radial proximity 4 connectivity (right).

librium - in that while individual agents continue to cycle through their individual states, the system as a whole reaches a statistical mean about which spatial regions fluctuate. The connectivity affects these fluctuations and there is scope to make a more detailed study of the fluctuation time and spatial size scales. This will affect how a widespread epidemic can continue to sustain itself or how it might be quenched or cut-off by introducing physical restrictions on physical infected component regions.

In addition to the expected monotonic behaviours from changes in the infection probability we have also seen cross over behaviours that are related to initial densities of infected and recovering agents. We have identified critical values of the infection and recovery parameters and there is scope to refine these statistically for larger model sizes of any particular lattices and geometries of interest.

We have explored a relatively simple model with one sort of infection present. A system with multiple diseases will likely have a more complex parametric structure as becoming infected or recovering from one sort of infection may change the susceptibility and exposure profile of agents to another. There is scope for incorporating this effect as well as more realistic geographic and exposure connectivity details. We believe exploring the parameter space of such models will be important in planning and "what-if" analyses for spatial epidemic models and this approach will continue to be useful for health planning - particularly in geographically land-locked regions where localised cross-infection is dominant.

References

[1] Arashiro, E., Tome, T.: The threshold of coexistence and critical behaviour of a predator-prey cellular automaon. J. Phys. A. Math. and Gen. 40, 887–900 (2007)

[2] Athithan, S., Shukla, V.P., Biradar, S.R.: Dynamic cellular automata based epidemic spread model for population in patches with movement. Journal of Computational Environmental Science A, 518053–1–8 (2014)

[3] Carduy, J.L., Grassberger, P.: Epidemic models and percolation. J. Phys. A Math. Gen. 18, L267–L271 (1985)

[4] pada Das, K., Kundu, K., Chattopadadhyay, J.: A predator-prey mathematical model with both the populations affected by diseases. Ecological Complexity 8, 68–80 (2011)

[5] Fuks, H., Lawniczak, A.T.: Individual-based lattice model for spatial spread of epidemics. Discrete Dynamics in Nature and Society 6, 191–200 (2001)

[6] Grassberger, P.: On the critical behavior of teh general epidemic process and dynamical percolation. Mathematical Biosciences 63, 157–172 (1983)

[7] Hawick, K.A.: Spectral analysis of growth in spatial lotka-volterra models. In: Proc. International Conference on Modelling and Simulation. pp. 14–20. No. 685-030, IASTED, Gabarone, Botswana (6-8 September 2010)

[8] Hawick, K.A.: Complex Domain Layering in Even Odd Cyclic State Rock-Paper-Scissors Game Simulations. In: Proc. IASTED International Conference on Modelling and Simulation (MS2011). pp. 129–136. No. 735-062, IASTED, Calgary, Alberta, Canada (4-6 July 2011)

[9] Hawick, K.A.: Cycles, diversity and competition in rock-paper-scissors-lizard-spock spatial game simulations. In: Proc. International Conference on Artificial Intelligence (ICAI'11). pp. 115–121. CSREA, Las Vegas, USA (18-21 July 2011)

[10] Hawick, K.A.: Catalytic sets and cyclic repetition in spatial agent-based models. Tech. Rep. CSTN-195, Computer Science, Massey University, Auckland, New Zealand (June 2013)

[11] Hawick, K.A.: Neighbourhood and number of states dependence of the transient period and cluster patterns in cyclic cellular automata. In: Proc. 10th Int. Conf. on Scientific Computing (CSC'13). p. CSC7339. No. CSTN-207, WorldComp, Las Vegas, USA (22-25 July 2013), `http://www.massey.ac.nz/~kahawick/cstn/207/cstn-207.html`

[12] Hawick, K.A., Scogings, C.J.: Dynamical runaway growth and simulation of cancer amongst spatial ani-

mat agents. In: IASTED Int. Conference on Applied Simulation and Modelling, Palma de Mallorca, Spain. pp. 142–147. Palma de Mallorca, Spain (7-9 September 2009), 682-011

[13] House, T., Keeling, M.J.: Deterministic epidemic models with explicit household structure. Mathematical Biosciences 213, 29–39 (2008)

[14] Husselmann, A.V., Hawick, K.A.: Genetic programming using the karva gene expression language on graphical processing units. In: Proc. 10th International Conference on Genetic and Evolutionary Methods (GEM'13). p. GEM2456. No. CSTN-171, WorldComp (22-25 July 2013)

[15] Jensen, I., Dickman, R.: Time dependent perturbation theory for diffusive non-equilibroium lattice models. J. Phys. A: Math. Gen. 26, L151–L157 (1993)

[16] Lalley, S.P., Perkins, E.A., Zheng, X.: A phase transition for measure-valued sir epidemic processes. The Annals of Probability 42, 237–310 (2014)

[17] Li, W.T., Lin, G., Ma, C., Yang, F.Y.: Traveling wave solutions of a nonlocal delayed sir model without outbreak threshold. Discrete and Continuous Dynamical Systems Series B 19(2), 467–484 (2014)

[18] Llensa, C., Juher, D., Saldana, J.: On the early epidemic dynamics for pairwise models. J. Theor. Biol. Online, 1–11 (2014)

[19] Matsuda, H., Ogita, N., Sasaki, A., Ka: Statistical mechanics of population. Progress of Theoretical Physics 88(6), 1035–1049 (1992)

[20] Moore, C., Newman, M.E.J.: Epidemics and percolation in small-world networks. SFI WORKING PAPER: 2000-01-002, Santa Fe Institute (2000)

[21] Moreira, A.G., Dickman, R.: Critical dynamics of the contact process with quenched disorder. Phys. Rev. E 54(4), R3090–R3093 (1996)

[22] de Oliveira, M.M., Alves, S.G., Ferreira, S.C., Dickman, R.: Contact process on a voronoi triangulation. Phys. Rev. E 78, 031133–1–5 (2008)

[23] Pan, Q., Liu, R., He, M.: An epidemic model baed on individuals with movement characteristics. Physica A 399, 157–162 (2014)

[24] Quach, D.Q., Willemse, J.M., Preez, V.D., Hawick, K.A.: Species survivability and altitude dependence in a lotka-volterra predator-prey spatial-agent based system. In: Proc. 14th Int. Conf. on Bioinformatics and Computational Biology. p. BIC7290. No. CSTN-231, WorldComp, Las Vegas, USA (22-25 July 2013), http://www.massey.ac.nz/~kahawick/cstn/231/cstn-231.html

[25] Rhodes, C.J., Anderson, R.M.: Dynamics in a lattice epidemic model. Physics Letters A 210, 183–188 (1996)

[26] Rhodes, C.J., Anderson, R.M.: Persistence and dynamics in lattice models of epidemic spread. J. Theor. Biol. 180, 125–133 (1996)

[27] Roberts, M.: The immunoepidemiology of nematode parasites of farmed animals: A mathematical approach. Parasitology Today 15(6), 246–251 (1999)

[28] Sabag, M.M.S., de Oliveira, M.J.: Conserved contact process in one to five dimensions. Phys. Rev E 66, 036115–1–5 (2002)

[29] Sazonov, I., Kelbert, M., Gravenor, M.B.: A new view on migration processes between sir centra: an account of the different dynamics of host and guest. arXiv 1401.6830v1, Swanse University (27 January 2014)

[30] de Souza, D.R., Tome, T.: Stochastic lattice gas model describing the dynamics of the sirs epidemic process. Physica A 389, 1142–1150 (2010)

[31] Tokar, V.I., Dreysse, H.: A lattice gas model of strained epitaxy and self-organization of small clusters. Computational Materials Science 24, 72–77 (2002)

[32] Tome, T., Ziff, R.M.: On the critical behavior of the susceptible-infected-recovered (sir) model on a square lattice. arXiv 1006.2129v2, Iniversidade de Sao Paulo, Brazil (27 October 2010)

[33] Wang, J., Liu, M., Li, Y.: Analysis of epidemic models with demographics in metapopulation networks. Physica A 392, 1621–1630 (2013)